

# Preparation, luminescent properties of *N*-phenyl-2-{2'-[(phenyl-ethyl-carbamoyl)-methoxy]-biphenyl-2-yloxy}-*N*-ethyl-acetamide (**L**) lanthanide complexes and the supramolecular structures of [La(pic)<sub>3</sub>L] and 2[La(NO<sub>3</sub>)<sub>3</sub>L(H<sub>2</sub>O)] · H<sub>2</sub>O · 0.5C<sub>2</sub>H<sub>5</sub>OH

Yan-Ling Guo<sup>a</sup>, Wei Dou<sup>a</sup>, Ya-Wen Wang<sup>a</sup>, Wei-Sheng Liu<sup>a,b,\*</sup>, Da-Qi Wang<sup>c</sup>

<sup>a</sup> Department of Chemistry and State Key Laboratory of Applied Organic Chemistry, Lanzhou University, Lanzhou 210093, China

<sup>b</sup> State Key Laboratory of Coordination Chemistry, Nanjing University, Nanjing 730000, China

<sup>c</sup> Department of Chemistry, Liaocheng University, Liaocheng 252000, China

Received 21 October 2006; accepted 6 December 2006

Available online 21 December 2006

## Abstract

A new amide-based ligand, *N*-phenyl-2-{2'-[(phenyl-ethyl-carbamoyl)-methoxy]-biphenyl-2-yloxy}-*N*-ethyl-acetamide (**L**) was synthesized. Solid complexes of lanthanide picrates with this new ligand were prepared and characterized by elemental analysis, conductivity measurements, IR, electronic and <sup>1</sup>H NMR spectroscopies. Under excitation, the europium picrate complex exhibited strong characteristic emissions. The europium nitrate complex exhibited quite weak characteristic emissions. The counter anion factor influencing the fluorescence properties was discussed. The lowest triplet state energy level of the ligand in the picrate complex matches better to the resonance level of Eu(III) than Tb(III) ion. The crystal structures of the complex La(Pic)<sub>3</sub>L and 2[La(NO<sub>3</sub>)<sub>3</sub>L(H<sub>2</sub>O)] · H<sub>2</sub>O · 0.5C<sub>2</sub>H<sub>5</sub>OH have been determined by single-crystal X-ray diffraction. The La(Pic)<sub>3</sub>L crystal structure shows that the La(III) ion is coordinated with four oxygen atoms from the ligand **L** and six from three bidentate picrates. Furthermore, the La(Pic)<sub>3</sub>L complex units are linked by the significant intermolecular π–π interactions between coordinate picrates to form a one-dimensional (1-D) supramolecular zigzag chain. The 2[La(NO<sub>3</sub>)<sub>3</sub>L(H<sub>2</sub>O)] · H<sub>2</sub>O · 0.5C<sub>2</sub>H<sub>5</sub>OH crystal structure shows that **L** gives two different arrangements around La(III) ions and induces axial chirality directed by metal ions in the assembly process of the organic ligands with metal ions, each La(III) ion is coordinated with four oxygen atoms from the ligand **L**, six oxygen atoms from three bidentate nitrate groups and one coordinate water molecule. Furthermore, the [La(NO<sub>3</sub>)<sub>3</sub>L(H<sub>2</sub>O)] complex units are linked by the intermolecular hydrogen bonds and π–π interaction to form a three-dimensional (3-D) netlike supramolecule.

© 2006 Elsevier Ltd. All rights reserved.

**Keywords:** Lanthanide complexes; Luminescent properties; Supramolecular structure; π–π Interaction; Hydrogen bonds

## 1. Introduction

Over the past decades, considerable attention has been devoted to the design and synthesis of luminescent lanthanide complexes due to their interesting photophysical properties, which have potential applications in sensors, liquid

crystalline materials, optical fiber lasers and amplifiers, luminescent label design for specific biomolecule interactions, magnetic molecular materials and electroluminescent materials [1–6].

Amide-based open-chain crown ethers offer many advantages in extraction and analysis of the rare earth ions because of their ring-like coordination structure and terminal group effects [7,8]. However, luminescent properties on open-chain crown ethers with lanthanide complexes have

\* Corresponding author. Tel.: +86 931 8912552; fax: +86 931 8912582.  
E-mail address: [liuws@lzu.edu.cn](mailto:liuws@lzu.edu.cn) (W.-S. Liu).

been rarely reported [9]. Our group is interested in the supramolecular coordination chemistry of lanthanide ions with amide-based open-chain crown ethers that have strong coordination capability to the lanthanide ions and terminal group effects [10]. So we have designed a series of multi-functional amide-based open-chain crown ethers having the ability to coordinate lanthanide ions and thus enhance luminescence of lanthanide complexes by providing chromophores suitable for energy transfer, i.e., aryl substitutes.

In this work, we introduced biphenyl groups as the basic molecular frame and obtained a new open-chain crown ether ligand, *N*-phenyl-2-{2'-[(phenyl-ethyl-carbamoyl)-methoxy]-biphenyl-2-yloxy}-*N*-ethyl-acetamide (**L**), and reported the synthesis, luminescent properties of lanthanide complexes with the new ligand and the supramolecular structures of La(pic)<sub>3</sub>L and 2[La(NO<sub>3</sub>)<sub>3</sub>L(H<sub>2</sub>O)]·H<sub>2</sub>O·0.5C<sub>2</sub>H<sub>5</sub>OH. The results indicate that under excitation, the Eu(III) picrate complex had strong characteristic luminescence whereas the terbium picrate complex showed no luminescence. The lowest triplet state energy level of the ligand in the picrate complex which was calculated from the phosphorescence spectrum of the Gd(III) picrate complex at 77 K, and indicates that the triplet state energy level of the ligand matches better to the resonance level of Eu(III) than Tb(III) ion. The Eu(III) nitrate complex exhibited quite weak characteristic emissions. The La(Pic)<sub>3</sub>L crystal structure shows that the La(III) ion could be effectively encapsulated and protected by the coordinated ligand. Furthermore, the La(Pic)<sub>3</sub>L complex units are linked by the significant intermolecular π–π interactions between coordinate picrates to form a one-dimensional (1-D) supramolecular zigzag chain. The 2[La(NO<sub>3</sub>)<sub>3</sub>L(H<sub>2</sub>O)]·H<sub>2</sub>O·0.5C<sub>2</sub>H<sub>5</sub>OH crystal structure shows that **L** gives two different arrangements around La(III) ions, and induces axial chirality directed by metal ions in the self-assembly process. Each La(III) ion is coordinated with four oxygen atoms from the ligand **L**, six oxygen atoms from three bidentate nitrate groups and one coordinate water molecule. Furthermore, the [La(NO<sub>3</sub>)<sub>3</sub>L(H<sub>2</sub>O)] complex units are linked by the intermolecular hydrogen bonds and π–π interaction to form a three-dimensional (3-D) netlike supramolecule.

## 2. Experimental

### 2.1. Materials

Lanthanide picrate [11] and *N*-ethyl-*N*-phenylchloroacetamide [12] were prepared according to the literature methods. All commercially available chemicals were of A.R. grade and were used without further purification.

### 2.2. Methods

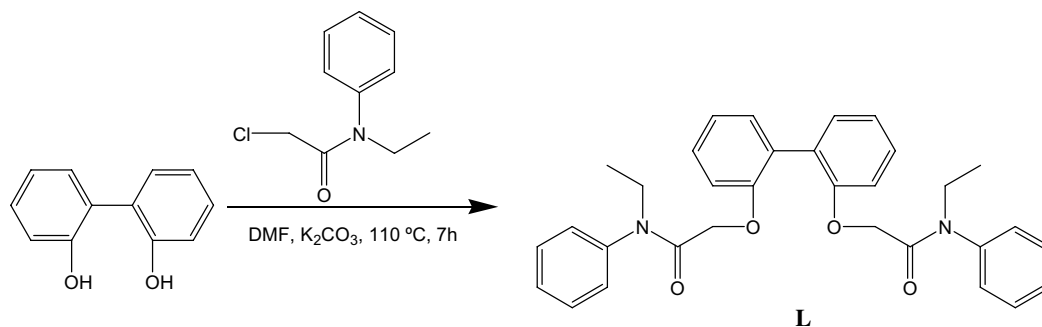
The metal ions were determined by EDTA titration using xylenal orange as indicator. C, H and N were determined using an Elementar Vario EL. Conductivity measurements were carried out with a DDS-307 type conductivity bridge using 10<sup>-3</sup> mol dm<sup>-3</sup> solutions at 25 °C. IR spectra were recorded on Nicolet FT-170SX instrument using KBr discs in the 400–4000 cm<sup>-1</sup> region, <sup>1</sup>H NMR spectra were measured on a Varian Mercury plus 300 M spectrometer in CDCl<sub>3</sub> solution with TMS as internal standard. Fluorescence and phosphorescence measurements were made on a Hitachi F-4500 spectrophotometer. Mass spectra were obtained on a VG-ZAB-HS mass spectrometer.

### 2.3. Synthesis of the ligand

The synthetic route for the ligand is shown in Scheme 1. Anhydrous K<sub>2</sub>CO<sub>3</sub> (5.6 g, 41 mmol) was added into the 15 mL DMF solution of 2,2'-dihydroxybiphenyl (1.86 g, 10 mmol) at 100 °C. After 1 h, a solution of *N*-ethyl-*N*-phenylchloroacetamide (5.92 g, 30 mmol) in 10 mL DMF was added dropwise to the mixture and maintained at 110 °C for 7 h. When cool, distilled water (60 ml) was added and the turbid solution was extracted with chloroform (3 × 40 mL). The combined organic phases were washed with water and dried with anhydrous Na<sub>2</sub>SO<sub>4</sub>. The solvent was removed and the residue was chromatographed to afford the ligand **L**; yield: 85%.

### 2.4. Synthesis of the lanthanide picrate complexes

To a solution of 0.2 mmol lanthanide picrate in 5 ml of ethanol was added dropwise the solution of 0.2 mmol **L** in



Scheme 1. The synthetic route for the ligand **L**.

10 ml of ethanol. The mixture was stirred at room temperature for 5 h. The precipitated solid complex was filtered, washed with ethanol and dried in vacuum over  $P_2O_5$  for 48 h. All the complexes were obtained as yellow powders in a yield of 80–85%. Slowly evaporating a solution of the lanthanum complex in  $CHCl_3/CH_3CH_2OH$  at room temperature, resulted in the formation of block crystals after 2 weeks.

### 2.5. Synthesis of the lanthanide nitrate complex

To a solution of 0.2 mmol lanthanide lanthanide nitrate in 5 ml of ethanol was added dropwise the solution of 0.2 mmol **L** in 10 ml of ethanol. The mixture was stirred at room temperature for 10 h and a clear solution obtained. The clear solution of lanthanum nitrate complex was filtered and left to crystallise. After about a month, a colorless crystal formed from the solution. After solvent evaporation from the solution of europium nitrate complex in vacuum, a white precipitate obtained, washed with little ethanol and dried in vacuum over  $P_2O_5$  for 72 h.

### 2.6. Crystal structure determination

X-ray diffraction data of  $La(pic)_3L$  and  $2[La(NO_3)_3L \cdot (H_2O)] \cdot H_2O \cdot 0.5C_2H_5OH$  were collected on a Bruker Smart-1000 CCD area detector diffractometer, using graphite-monochromatized  $Mo\ K\alpha$  ( $\lambda = 0.71073\text{ \AA}$ ) at 298(2) K. The structures were solved by direct method and refined by full matrix least-squares techniques on  $F^2$  with all non-hydrogen atoms treated anisotropically. All calculations were performed with the program package SHELXTL. The hydrogen atoms were assigned with common isotropic displacement factors and included in the final refinement by using geometrical restraints.

## 3. Results and discussion

### 3.1. Properties of the complexes

Analytical data for the complexes, listed in Table 1, indicate that the seven complexes of rare earth picrates and europium nitrate conform to a 1:1 metal-to-ligand stoichiometry  $Ln(pic)_3L$  and  $Eu(NO_3)_3L$ . All the picrate complexes are soluble in DMF, DMSO, acetonitrile, acetone and  $CHCl_3$ , but slightly soluble in ethanol. The molar con-

ductances of the picrate complexes in acetone and  $Eu(NO_3)_3L$  in DMF (see Table 1) indicate that all the picrate complexes and  $Eu(NO_3)_3L$  act as non-electrolytes [13], implying that all the picrate groups and nitrate groups are in the coordination sphere.

### 3.2. Crystal structure of $La(Pic)_3L$

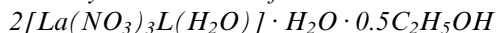
A summary of crystallographic data and details of the structure refinements are listed in Table 2. The selected bond lengths and bond angles are given in Table 3.

The single-crystal X-ray analysis of the complex  $La(Pic)_3L$  reveals that the La(III) ion is coordinated with 10 oxygen donor atoms, six of which belong to three bidentate picrate groups and the remaining four to the tetradentate ligand **L** (Fig. 1). The coordination polyhedron around La(III) ion is a distorted bicapped square antiprism (Fig. 2). The two phenyl rings about the central bond in the molecule have a drastic twisting, with the dihedral angle between them being  $62.49^\circ$ . The La–O (C=O) distances (mean 2.461 Å) are significantly shorter than the La–O (C–O–C) distances (mean 2.701 Å). This suggests that the La–O (C=O) bond is stronger than the La–O (C–O–C) bond.

In the complex, the requirement of high coordination number of the lanthanide ion is satisfied by the tetradentate ligand and three bidentate picrate groups. Due to the space obstacle of coordinated picrates, no coordinated solvent molecules exist in the complex, which can efficiently quench lanthanide luminescence, this is important in the design of supramolecular photonic devices.

Interestingly, the complex has significant intermolecular  $\pi$ – $\pi$  interaction [14] between two picrates of one complex molecule and equivalent picrates of the adjacent molecules with the dihedral angles between them being  $0^\circ$  and  $0^\circ$ , and the distances between their centroids being 3.774, 4.019 Å, respectively, thus, producing a one-dimensional (1-D) supramolecular zigzag chain (Fig. 3).

### 3.3. Crystal structure of



A summary of crystallographic data and details of the structure refinements are listed in Table 2. The selected bond lengths and bond angles are given in Table 4.

Table 1  
Analytical and molar conductance data for the complexes (calculated values in parentheses)

Complex	Analysis (%)				$\Lambda_m$ ( $cm^2\ \Omega^{-1}\ mol^{-1}$ )
	C	H	N	Ln	
$La(pic)_3L$	44.78(45.08)	3.01(2.86)	11.43(11.57)	10.21(10.44)	34.0
$Nd(pic)_3L$	44.63(44.91)	3.04(2.84)	11.38(11.53)	10.53(10.78)	31.7
$Eu(pic)_3L$	44.17(44.64)	2.70(2.83)	11.32(11.46)	11.13(11.31)	29.8
$Gd(pic)_3L$	44.16(44.48)	2.94(2.82)	11.14(11.42)	11.28(11.64)	32.7
$Tb(pic)_3L$	44.12(44.41)	2.72(2.81)	11.26(11.40)	11.32(11.77)	31.2
$Y(pic)_3L$	46.56(46.84)	2.68(2.97)	12.08(12.02)	6.64(6.95)	34.6
$Eu(NO_3)_3L$	45.78(45.39)	3.08(3.78)	8.63(8.27)	17.49(17.97)	50.3

Table 2  
Crystal data and structure refinements for lanthanum picrate and lanthanum nitrate complexes

Empirical formula	C <sub>50</sub> H <sub>38</sub> LaN <sub>11</sub> O <sub>25</sub>	C <sub>65</sub> H <sub>73</sub> La <sub>2</sub> N <sub>10</sub> O <sub>29.50</sub>
Temperature (K)	298(2)	293(2)
Crystal color	yellow	colourless
Crystal size (mm)	0.45 × 0.38 × 0.19	0.53 × 0.48 × 0.45
Formula weight	1331.82	1744.15
Crystal system	triclinic	monoclinic
Space group	<i>P</i> $\bar{1}$	<i>P</i> 2(1)/ <i>c</i>
<i>Unit cell dimensions</i>		
<i>a</i> (Å)	10.9574(18)	25.733(8)
<i>b</i> (Å)	15.381(3)	11.978(4)
<i>c</i> (Å)	16.877(3)	28.383(8)
$\alpha$ (°)	95.734(3)	90
$\beta$ (°)	90.664(2)	116.452(4)
$\gamma$ (°)	107.748(2)	90
<i>V</i> (Å <sup>3</sup> )	2692.8(8)	7832(4)
<i>Z</i>	2	4
<i>D</i> <sub>calc</sub> (mg/m <sup>3</sup> )	1.643	1.479
<i>F</i> (000)	1344	3532
Radiation, graphite-monochromatized, $\lambda$ (Å)	0.71073	0.71073
Reflections collections	14193	39525
Independent reflection	9335	13698
$\theta$ Range for data collection (°)	1.95–25.01	1.92–25.01
Index range	−13 ≤ <i>h</i> ≤ 12 −9 ≤ <i>k</i> ≤ 18 −20 ≤ <i>l</i> ≤ 19	−28 ≤ <i>h</i> ≤ 30 −8 ≤ <i>k</i> ≤ 14 −33 ≤ <i>l</i> ≤ 33
Goodness-of-fit on <i>F</i> <sup>2</sup>	1.081	1.081
<i>R</i> [ <i>I</i> > 2 $\sigma$ ( <i>I</i> )]	<i>R</i> = 0.0519, <i>wR</i> = 0.1132	<i>R</i> = 0.0657, <i>wR</i> = 0.1641
<i>R</i> (all data)	<i>R</i> = 0.0825, <i>wR</i> = 0.1327	<i>R</i> = 0.1687, <i>wR</i> = 0.2313
Largest difference peak and hole [e Å <sup>−3</sup> ]	1.148, −0.612	1.388, −1.009

Table 3  
Selected bond lengths (Å) and bond angles (°) for La(pic)<sub>3</sub>L

La(1)–O(12)	2.404(4)	La(1)–O(3)	2.700(3)
La(1)–O(5)	2.419(4)	La(1)–O(1)	2.700(3)
La(1)–O(19)	2.423(4)	La(1)–O(20)	2.794(4)
La(1)–O(2)	2.429(3)	La(1)–O(13)	2.842(5)
La(1)–O(4)	2.492(3)	La(1)–O(6)	2.937(5)
O(2)–La(1)–O(4)	124.8(1)	O(3)–La(1)–O(1)	65.9(1)
O(4)–La(1)–O(3)	60.1(1)	O(19)–La(1)–O(20)	60.5(1)
O(2)–La(1)–O(1)	60.1(1)	O(12)–La(1)–O(13)	59.1(1)
O(4)–La(1)–O(1)	73.3(1)	O(5)–La(1)–O(6)	58.4(1)

The [La(NO<sub>3</sub>)<sub>3</sub>L(H<sub>2</sub>O)] · H<sub>2</sub>O · 0.5C<sub>2</sub>H<sub>5</sub>OH crystal structure reveals that there are two independent molecules in the unit cell. Each La(III) ion is coordinated with 11 oxygen donor atoms. Six of them belong to three bidentate nitrate groups, one of them belongs to one coordinate water molecule, and the remaining four are from the tetradentate ligand **L** (Fig. 4). Upon coordination, **L** gives two different arrangements (A and B) around La(III) ions in the unit cell. In structure A, the two phenyl rings about the central bond in the molecule have a drastic twisting, with the dihedral angle between them being 56.75°. Again, the La(1)–O (C=O) distances (mean 2.512 Å) are shorter than the La–O (C–O–C) distances (mean 2.764 Å), suggesting that La–O (C=O) bond is stronger than the La–O (C–O–C) bond. The same situation occurs in structure B, where the dihedral angle between the two phenyl rings in the molecule is 58.61°, the average distance between La(2) atom and oxygen atoms

(C=O) is 2.525 Å and the average distance between La(2) and oxygen atoms (C–O–C) is 2.781 Å. It is interesting that the free ligand is achiral, but upon metal coordination, it induces axial chirality. As shown in Fig. 4, the ligand exhibits (*S*) configuration in structure A and (*R*) configuration in structure B in the unit cell, which is contributed to the metal-directed self-assembly process of the ligands with the metal ions [15].

In structure A, atom O(14) acts as hydrogen bond donor to form O–H ···O with the oxygen atom O(12) of the adjacent equivalent molecule [O(12) ···H(68), 2.268 Å and O(14)–H(68) ···O(12), 144.34°], thus, generating a one-dimensional (1-D) supramolecular zigzag chain along the *b* axis as shown in Fig. 5a.

In structure B, atom C(51) acts as hydrogen bond donor to form C–H ···O with the oxygen atom O(22) of the adjacent equivalent molecule [O(22) ···H(51), 2.604 Å and C(51)–H(51) ···O(22), 134.33°] [16], thus, generating a dimer as shown in Fig. 5(b); furthermore, the dimeric blocks are linked by the intermolecular hydrogen bond O(28)–H(70) ···O(26) [O(26) ···H(70), 2.222 Å and O(28)–H(70) ···O(26), 150.84°] to form a two-dimensional (2-D) supramolecular layer with hydrogen bonded channels as shown in Fig. 5c and d.

In addition, intermolecular  $\pi$ – $\pi$  interaction [14] between one phenyl ring of one ligand frame from one chain and another phenyl ring of the adjacent ligand frame from the adjacent layer with the dihedral angle between them being 6.01° and the distance between their centroids being

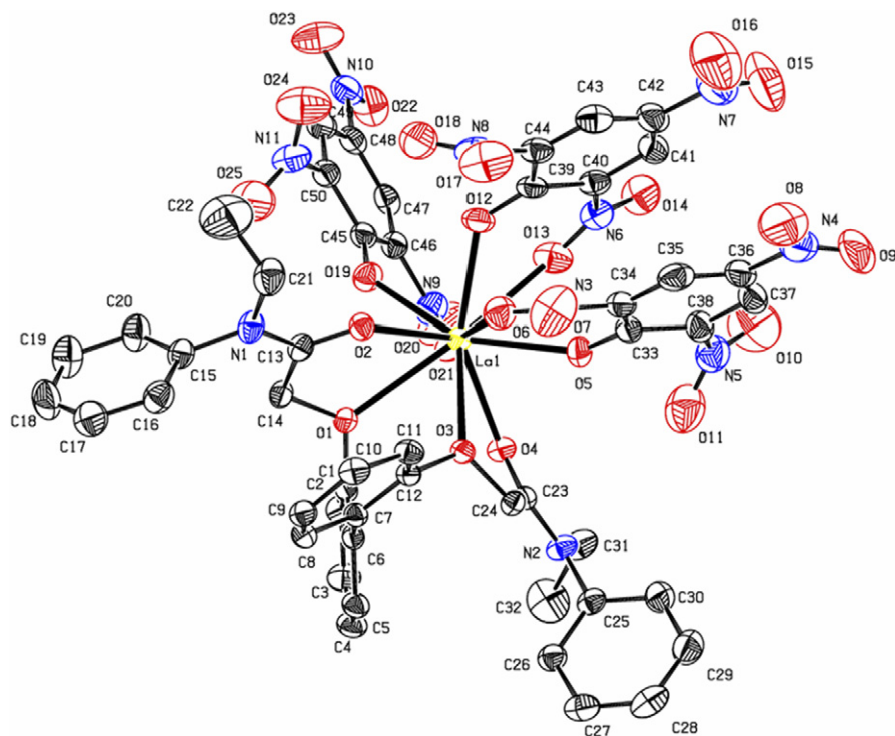


Fig. 1. ORTEP diagram (30% probability ellipsoids) showing the coordination sphere of  $[\text{La}(\text{pic})_3\text{L}]$ . Hydrogen atoms are omitted for clarity.

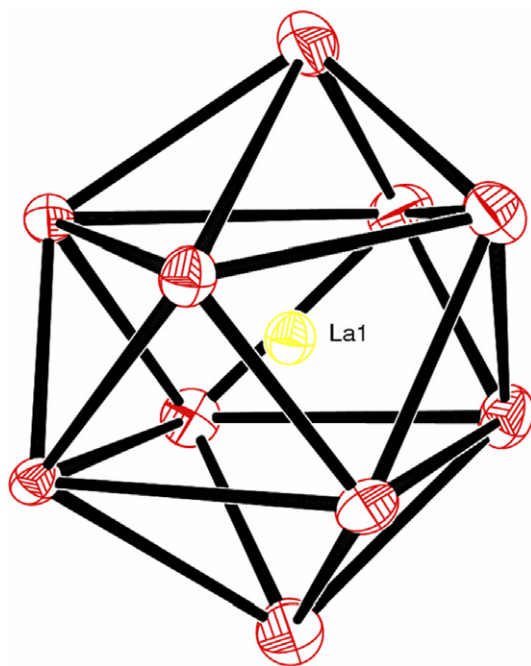


Fig. 2. Coordination polyhedron of La(III) ion in  $\text{La}(\text{pic})_3\text{L}$ .

4.058 Å, further produce a three-dimensional (3-D) netlike supramolecule as shown in Fig. 6.

### 3.4. IR spectra

The main infrared bands of the ligand and their complexes are presented in Tables 5 and 6. The “free” ligand

**L** exhibits two absorption bands at 1676 and 1126  $\text{cm}^{-1}$  which are assigned to  $\nu(\text{C}=\text{O})$  and  $\nu(\text{C}-\text{O}-\text{C})$ , respectively.

In picrate complexes, the  $\nu(\text{C}=\text{O})$  and  $\nu(\text{C}-\text{O}-\text{C})$  of the free ligand shift by ca. 57 and 46  $\text{cm}^{-1}$  towards lower wave numbers, thus indicating that the  $\text{C}=\text{O}$  and ether O-atoms take part in coordination to the metal ions.

The OH out-of-plane bending vibration of the free Hpic at 1151  $\text{cm}^{-1}$  disappears in the spectra of the complexes indicating that the H atom of the OH group is replaced by Ln(III) ions. The vibration  $\nu(\text{C}-\text{O})$  at 1265  $\text{cm}^{-1}$  is shifted towards higher frequency by ca. 10  $\text{cm}^{-1}$  in the complexes. This is due to the following two effects. First, the hydrogen atom of the OH group is replaced by Ln(III), increasing the  $\pi$ -bond character in the C–O bond. Secondly, coordination of the oxygen atom of **L** to Ln(III) causes the  $\pi$ -character to be weakened [10b]. The free Hpic has  $\nu_{\text{as}}(\text{NO}_2)$  and  $\nu_{\text{s}}(\text{NO}_2)$  at 1555 and 1342  $\text{cm}^{-1}$ , respectively, which splits into two bands at 1584, 1545  $\text{cm}^{-1}$  and 1352, 1331  $\text{cm}^{-1}$  in the complexes. This indicates that some of the O-atoms in the nitro group of  $\text{Pic}^-$  take part in coordination [17]. On the basis of the similarity of their IR spectra, it may be assumed that the picrate complexes have the similar structures.

In the europium nitrate complex, the  $\nu(\text{C}=\text{O})$  and  $\nu(\text{C}-\text{O}-\text{C})$  of the free ligand shift by ca. 50 and 54  $\text{cm}^{-1}$  towards lower wave numbers, thus indicating that all the  $\text{C}=\text{O}$  and ether O atoms take part in coordination to the metal ion. The absorption bands assigned to the coordinated nitrate groups ( $\text{C}_{2v}$ ) are observed at about 1495  $\text{cm}^{-1}$  ( $\nu_1$ ), 1308  $\text{cm}^{-1}$  ( $\nu_4$ ), 1030  $\text{cm}^{-1}$  ( $\nu_2$ ) and 815  $\text{cm}^{-1}$  ( $\nu_3$ ) [18] for the nitrate complex. In addition, the separation of the

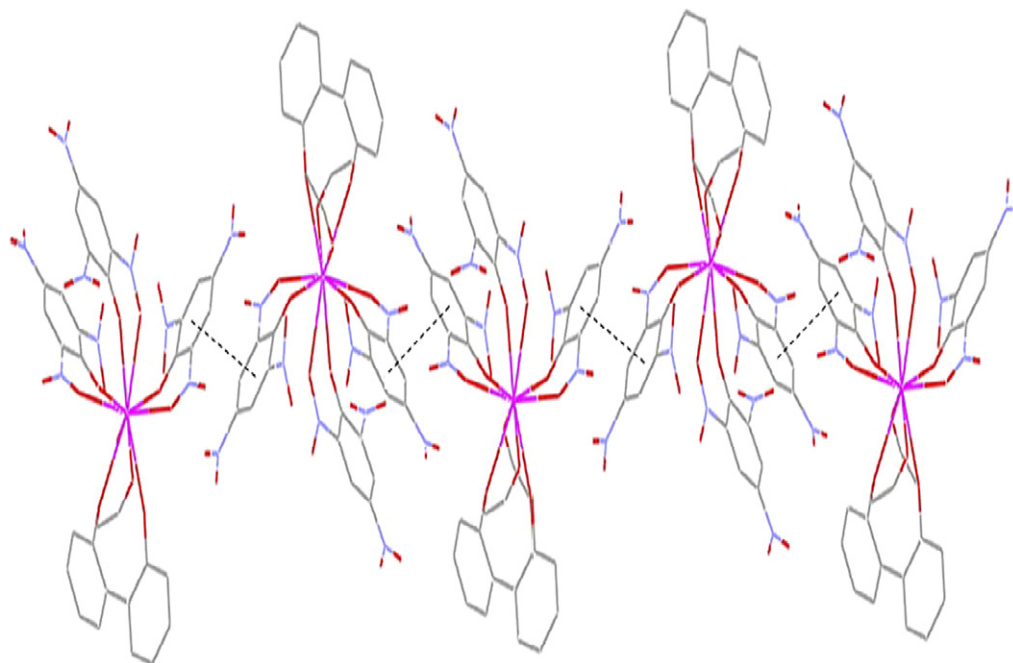


Fig. 3. The zigzag chain of  $[\text{La}(\text{pic})_3\text{L}]$  linked by intermolecular  $\pi$ - $\pi$  stacking interactions. All the *N*-ethylanilines are omitted for clarity.

Table 4

Selected bond lengths (Å) and bond angles (°) for  $2[\text{La}(\text{NO}_3)_3\text{L}(\text{H}_2\text{O})] \cdot \text{H}_2\text{O} \cdot 0.5\text{C}_2\text{H}_5\text{OH}$

La(1)–O(1)	2.492(7)	La(2)–O(15)	2.523(8)
La(1)–O(3)	2.532(7)	La(2)–O(17)	2.527(7)
La(1)–O(14)	2.538(7)	La(2)–O(28)	2.560(7)
La(1)–O(11)	2.636(8)	La(2)–O(22)	2.576(9)
La(1)–O(12)	2.639(7)	La(2)–O(20)	2.623(9)
La(1)–O(8)	2.646(8)	La(2)–O(19)	2.631(8)
La(1)–O(6)	2.649(9)	La(2)–O(26)	2.633(8)
La(1)–O(9)	2.662(8)	La(2)–O(25)	2.690(8)
La(1)–O(5)	2.715(9)	La(2)–O(23)	2.698(9)
La(1)–O(4)	2.722(6)	La(2)–O(18)	2.723(7)
La(1)–O(2)	2.807(7)	La(2)–O(16)	2.839(7)
O(1)–La(1)–O(3)	125.1(2)	O(15)–La(2)–O(17)	128.2(2)
O(1)–La(1)–O(14)	70.0(2)	O(15)–La(2)–O(28)	125.1(3)
O(3)–La(1)–O(14)	123.7(2)	O(17)–La(2)–O(28)	73.1(2)
O(11)–La(1)–O(12)	47.5(2)	O(20)–La(2)–O(19)	47.9(3)
O(8)–La(1)–O(9)	46.6(3)	O(26)–La(2)–O(25)	47.7(3)
O(6)–La(1)–O(5)	46.2(3)	O(22)–La(2)–O(23)	47.3(3)
O(1)–La(1)–O(4)	75.4(2)	O(15)–La(2)–O(18)	81.4(2)
O(3)–La(1)–O(4)	59.3(2)	O(17)–La(2)–O(18)	58.5(2)
O(14)–La(1)–O(4)	79.2(2)	O(28)–La(2)–O(18)	70.1(2)
O(1)–La(1)–O(2)	57.9(2)	O(15)–La(2)–O(16)	57.3(2)
O(3)–La(1)–O(2)	73.0(2)	O(17)–La(2)–O(16)	74.3(2)
O(14)–La(1)–O(2)	119.7(2)	O(28)–La(2)–O(16)	130.7(2)
O(4)–La(1)–O(2)	60.9(2)	O(18)–La(2)–O(16)	61.5(2)

two strongest frequencies  $|v_1 - v_4|$  is approximately  $187 \text{ cm}^{-1}$ , clearly establishing that the  $\text{NO}_3^-$  groups in the solid complex coordinate to the rare earth ion as bidentate ligands [19]. Also no bands at 1380, 820 and  $720 \text{ cm}^{-1}$  in the spectrum of complex indicates that free nitrate groups ( $D_{3h}$ ) are absent, in agreement with the result of the conductivity experiment.

### 3.5. $^1\text{H}$ NMR spectra and mass spectra

**L:**  $^1\text{H}$  NMR ( $\text{CDCl}_3$ ):  $\delta$  7.34–7.18(m, 10H, ArH and  $\text{C}_{12}\text{H}_8^-$ ), 7.07(q,  $J = 7.8 \text{ Hz}$ , 4H, ArH), 6.96(t,  $J = 7.5 \text{ Hz}$ , 2H, ArH), 6.73(d,  $J = 7.8 \text{ Hz}$ , 2H, ArH), 4.21(s, 4H,  $-\text{O}-\text{CH}_2-\text{CO}-$ ), 3.71(q,  $J = 7.2 \text{ Hz}$ , 4H,  $-\text{N}-\text{CH}_2-$ ), 1.08(t,  $J = 7.2 \text{ Hz}$ , 6H,  $-\text{CH}_3$ ).

$[\text{La}(\text{pic})_3 \cdot \text{L}]$ :  $^1\text{H}$  NMR ( $\text{CDCl}_3$ ):  $\delta$  8.94(s, 6H, pic-), 7.39–7.07(m, 18H, ArH and  $\text{C}_{12}\text{H}_8^-$ ), 4.45(d,  $J = 14.7 \text{ Hz}$ , 2H,  $-\text{O}-\text{CH}_2-\text{CO}-$ ), 4.09(d,  $J = 14.7 \text{ Hz}$ , 2H,  $-\text{O}-\text{CH}_2-\text{CO}-$ ), 3.51(q,  $J = 6.9 \text{ Hz}$ , 4H,  $-\text{N}-\text{CH}_2-$ ), 0.91(t,  $J = 6.9 \text{ Hz}$ , 6H,  $-\text{CH}_3$ ).

$[\text{Y}(\text{pic})_3 \cdot \text{L}]$ :  $^1\text{H}$  NMR ( $\text{CDCl}_3$ ):  $\delta$  8.84(s, 6H, pic-), 7.42–7.19(m, 18H, ArH and  $\text{C}_{12}\text{H}_8^-$ ), 4.80(d,  $J = 15.3 \text{ Hz}$ , 2H,  $-\text{O}-\text{CH}_2-\text{CO}-$ ), 4.11(d,  $J = 15.3 \text{ Hz}$ , 2H,  $-\text{O}-\text{CH}_2-\text{CO}-$ ), 3.51(q,  $J = 6.9 \text{ Hz}$ , 4H,  $-\text{N}-\text{CH}_2-$ ), 0.91(t,  $J = 6.9 \text{ Hz}$ , 6H,  $-\text{CH}_3$ ).

The  $^1\text{H}$  NMR spectra of the “free” ligand **L**, the diamagnetic Ln(III) picrate complexes  $\text{La}(\text{Pic})_3\text{L}$  and  $\text{Y}(\text{Pic})_3\text{L}$  were measured in  $\text{CDCl}_3$ . The spectrum of **L** exhibits a multiplet at ca. 7.26 ppm, a quadruplet at 7.07 ppm ( $J = 7.8 \text{ Hz}$ ), a triplet at 6.96 ppm ( $J = 7.5 \text{ Hz}$ ) and a doublet at 6.73 ppm ( $J = 7.8 \text{ Hz}$ ) assigned to  $\text{C}_{12}\text{H}_8^-$  and  $-\text{C}_6\text{H}_5$  protons, a singlet at 4.21 ppm, a quadruplet at 3.71 ppm ( $J = 7.2 \text{ Hz}$ ), and a triplet at 1.08 ppm ( $J = 7.2 \text{ Hz}$ ) assigned to  $-\text{O}-\text{CH}_2-\text{CO}-$  protons,  $-\text{N}-\text{CH}_2-$  protons,  $-\text{CH}_3$  protons, respectively.

Upon coordination, the proton signal of  $-\text{O}-\text{CH}_2-\text{CO}-$  in the lanthanum and yttrium complexes split into two doublets at 4.45 ppm ( $J = 14.7 \text{ Hz}$ ), 4.09 ppm ( $J = 14.7 \text{ Hz}$ ) and 4.80 ppm ( $J = 15.3 \text{ Hz}$ ), 4.11 ppm ( $J = 15.3 \text{ Hz}$ ), respectively. The signal of  $-\text{N}-\text{CH}_2-$  and  $-\text{CH}_3$  are shifted to higher field by 0.20 and 0.17 ppm, respectively. The reason is not clear.

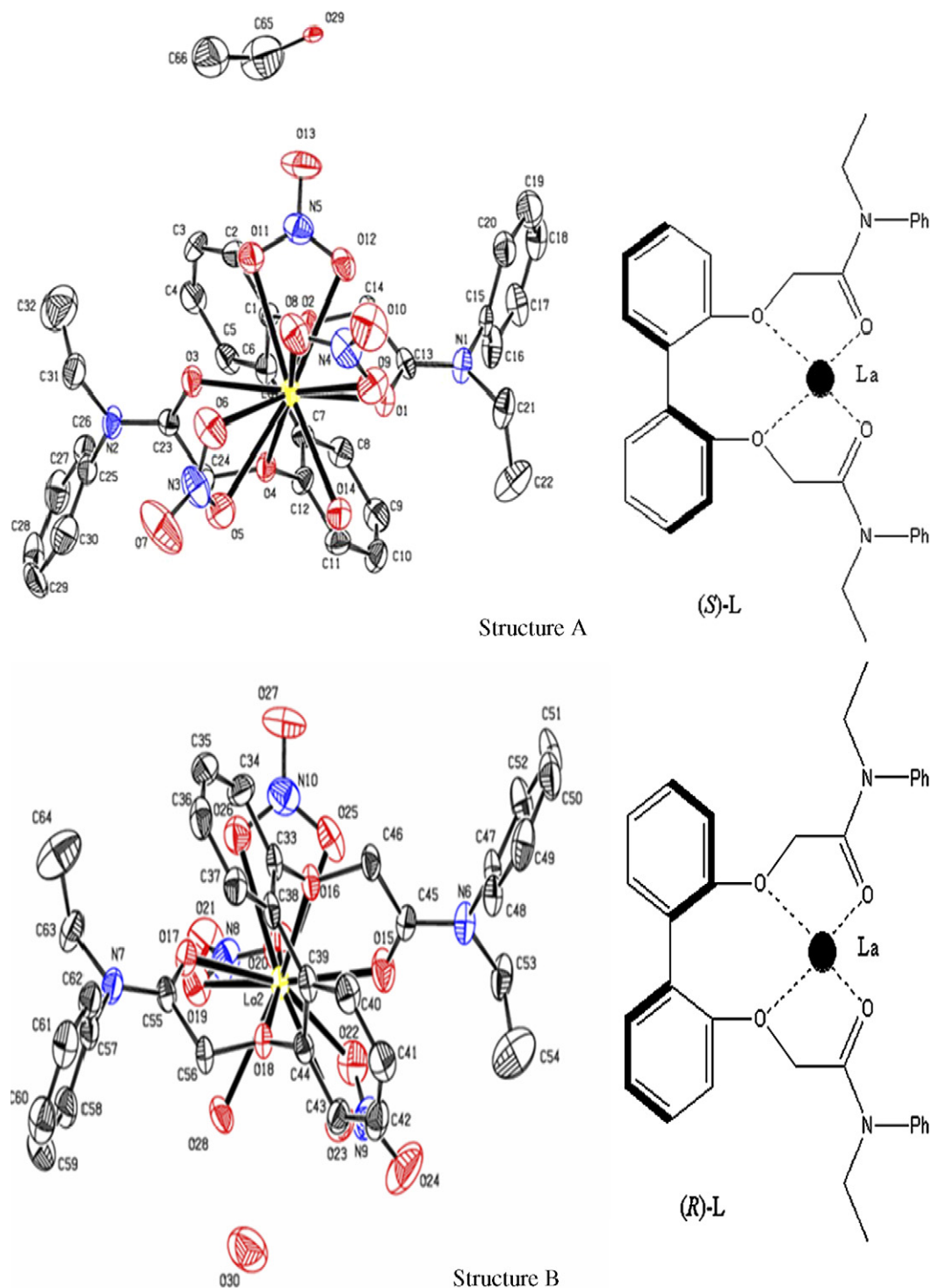


Fig. 4. ORTEP diagram (30% probability ellipsoids) showing the coordination sphere of  $[\text{La}(\text{NO}_3)_3\text{L}(\text{H}_2\text{O})]$  and coordination modes of L in the nitrate complex.

The proton signal of the OH group in free HPic disappears in the complexes, indicating that the H atom of the OH group is replaced by Ln(III). The benzene ring protons of the free HPic exhibit a singlet at 9.12 ppm. Upon coordination, the signal moves to higher field. Only one singlet is observed for the benzene ring protons of the three coordination picrate groups, indicating fast exchange among the groups in solution [20].

The mass spectrum of L shows a molecular ion at  $m/z = 509$  ( $M + H$ ), confirming the molecular formula of L as  $\text{C}_{32}\text{H}_{32}\text{N}_2\text{O}_4$ . Above the mass of  $\text{C}_{12}\text{H}_8$  ( $m/z = 152$ ) are observed three major fragment ions at  $m/z = 360$  ( $M - [-\text{CO}-\text{NC}_6\text{H}_5(\text{C}_2\text{H}_5)]$ ), 330 ( $M - [-\text{O}-\text{CH}_2-\text{CO}-\text{NC}_6\text{H}_5(\text{C}_2\text{H}_5)]$ ), and 181 ( $M - [-\text{O}-\text{CO}-\text{NC}_6\text{H}_5(\text{C}_2\text{H}_5)] - [-\text{O}-\text{CH}_2-\text{CO}-\text{NC}_6\text{H}_5(\text{C}_2\text{H}_5)]$ ).

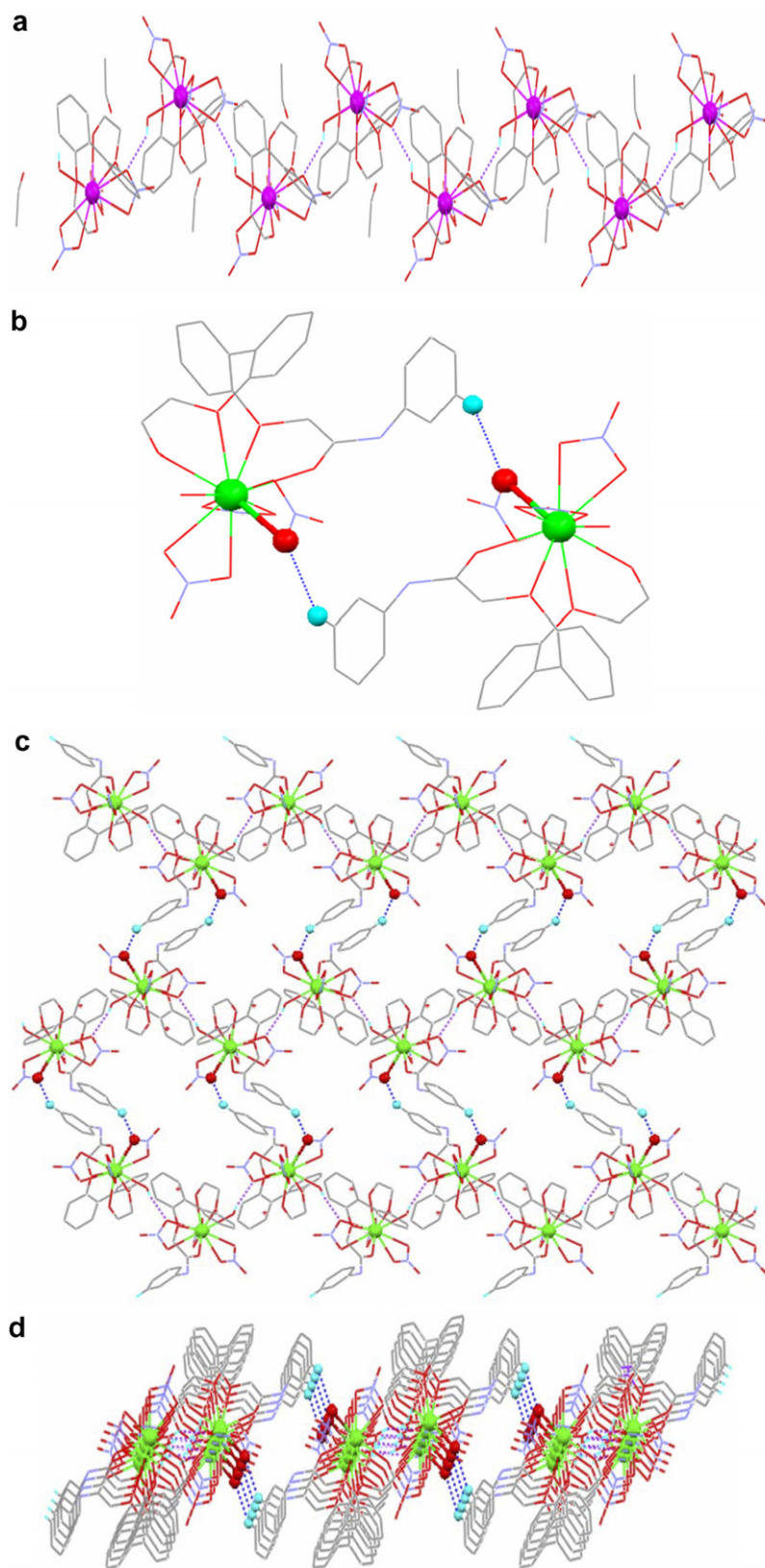


Fig. 5. Hydrogen bonding architecture in lanthanum nitrate complex: (a) 1-D zigzag chain of structure A generated by intermolecular O(14)–H(68)···O(12) hydrogen bonds [symmetry code is  $-x, -1/2 + y, 1/2 - z$ ; and the hydrogen bonds are indicated by the purple dashed lines]; (b) the dimer of structure B generated by intermolecular C(51)–H(51)···O(22) hydrogen bonds [symmetry code is  $1 - x, 2 - y, 1 - z$ ; and the hydrogen bonds are indicated by the blue dashed lines]; (c) 2-D layer of structure B generated by intermolecular O(28)–H(70)···O(26) hydrogen bonds [symmetry code is  $1 - x, 1/2 + y, 1/2 - z$ ; and the hydrogen bonds are indicated by the purple dashed lines] and C(51)–H(51)···O(22) hydrogen bonds (the hydrogen bonds are indicated by the blue dashed lines); (d) 2-D layer of structure B viewed down the crystallographic *b*-axis showing the hydrogen bonded channels. Some atoms of the ligand are omitted for clarity.

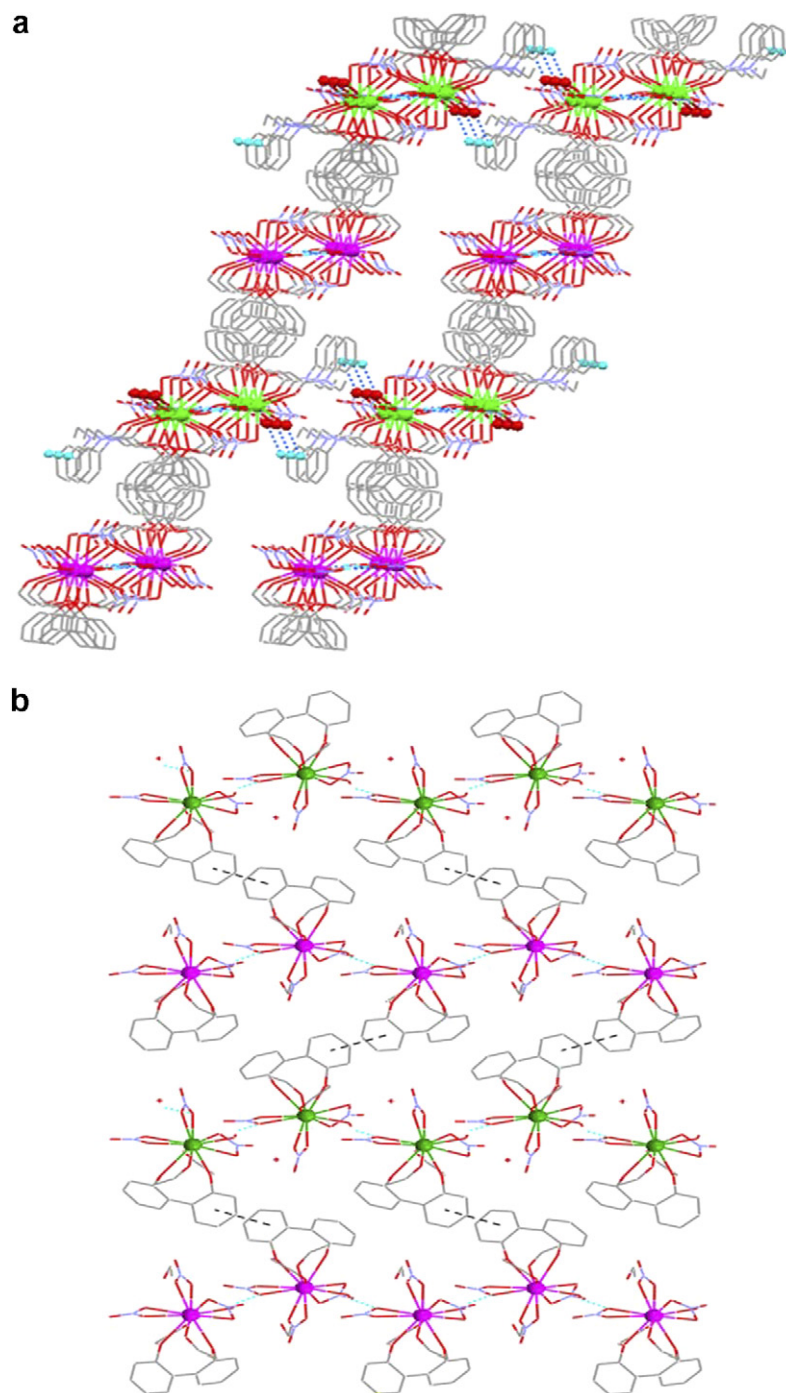


Fig. 6. The intermolecular  $\pi$ - $\pi$  stacking interactions between the chains and the layers in lanthanum nitrate complex: (a) viewing of the packing diagram of networks along the  $b$ -axis; (b) packing diagram of the chains and the layers along  $a$ -axis. Some atoms of the ligand are omitted for clarity.

### 3.6. Electronic spectra

The electronic spectra in the visible region of the Ln(III) complexes exhibit alternations in intensity and shifts in position of the absorption bands relative to the corresponding Ln(III) aquo ions. The shift has been attributed by Jorgensen to the effect on the crystal field of interelectronic repulsion between the 4f electrons, and is related to the

covalent character of the metal–ligand bond, assessed by Sinha's parameter ( $\delta$ ), the nephelauxetic ration ( $\beta$ ) and the bonding parameter ( $b^{1/2}$ ) [21]. Absorption spectrum of the Nd(III) complex was recorded in chloroform solution at room temperature and the covalent parameters were calculated (Table 7). The values of  $\beta$ , which are less than unity, and positive values of  $\delta$  and  $b^{1/2}$  support the existence of partial covalent bonding between metal and ligand [22].

Table 5  
The most important IR bands of the rare earth picrate complexes ( $\text{cm}^{-1}$ )

Complex	$\nu(\text{C}=\text{O})$	$\nu(\text{C}-\text{O}-\text{C})$	$\nu(\text{C}-\text{O})$	$\nu_{\text{as}}(-\text{NO}_2)$	$\nu_{\text{s}}(-\text{NO}_2)$
Hpic			1265	1555	1342
L	1676	1126			
La(pic) <sub>3</sub> L	1618	1080	1274	1584, 1545	1359, 1330
Nd(pic) <sub>3</sub> L	1617	1081	1276	1584, 1545	1358, 1329
Eu(pic) <sub>3</sub> L	1619	1079	1275	1585, 1541	1352, 1331
Gd(pic) <sub>3</sub> L	1619	1081	1275	1577, 1541	1352, 1332
Tb(pic) <sub>3</sub> L	1618	1081	1279	1586, 1547	1357, 1328
Y(pic) <sub>3</sub> L	1620	1080	1274	1578, 1542	1352, 1333

Table 6  
The most important IR bands of europium nitrate complexes ( $\text{cm}^{-1}$ )

Complex	$\nu(\text{C}=\text{O})$	$\nu(\text{C}-\text{O}-\text{C})$	$\nu(\text{NO}_3^-)$				
			$\nu_1$	$\nu_2$	$\nu_3$	$\nu_4$	$ \nu_1-\nu_4 $
L	1676	1126					
Eu(NO <sub>3</sub> ) <sub>3</sub> L	1626	1072	1495	1030	815	1308	187

Table 7  
Covalent parameters for the neodymium picrate complex

Complex	Frequency ( $\text{cm}^{-1}$ )	Assignment	Covalent parameters
Nd(pic) <sub>3</sub> L	11429	$^4\text{I}_{9/2} \rightarrow ^4\text{F}_{3/2}$	$\beta = 0.9999$
	12453	$^4\text{F}_{5/2}$	$\delta = 0.0100$
	13387	$^4\text{F}_{7/2}$	$b^{1/2} = 0.0071$
	13531	$^4\text{S}_{3/2}$	
	17182	$^4\text{G}_{5/2}$	
	17421	$^2\text{G}_{7/2}$	
	19048	$^4\text{G}_{7/2}$	

### 3.7. Fluorescence studies

Monitored by the emission band at 600 nm, the europium picrate complex exhibits broad excitation bands around 450 nm. The luminescence emission spectra of the europium picrate complex in solid state (the excitation and emission slit widths were 1.0 nm, Fig. 7) and in solu-

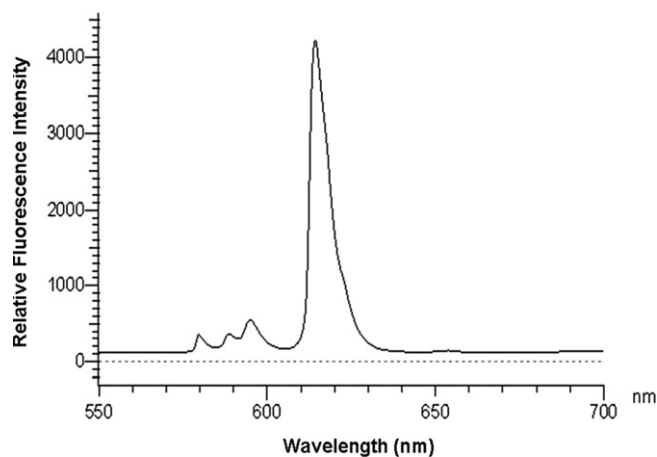


Fig. 7. The emission spectrum of the europium picrate complex in solid state.

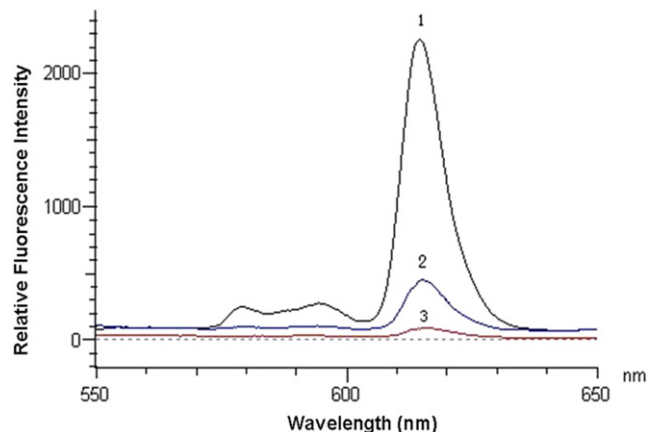


Fig. 8. The emission spectrum of the europium picrate complex in different solutions at room temperature: (1) in  $\text{CHCl}_3$ , (2) in acetone, and (3) in acetonitrile solution.

tion (the excitation and emission slit widths were 5.0 nm, Fig. 8) were recorded at room temperature. The luminescence characteristics of the europium picrate complex in solid state and in  $\text{CHCl}_3$ , acetone, acetonitrile, and DMF solutions (concentration:  $1.0 \times 10^{-3} \text{ mol L}^{-1}$ ) are listed in Table 8. It can be seen that the europium picrate complex shows strong emission when excited with 451 nm in the solid state. The highest intensity ratio value  $\eta(^5\text{D}_0 \rightarrow ^7\text{F}_2/^5\text{D}_0 \rightarrow ^7\text{F}_1)$  is 7.7, indicative of the Eu(III) ion not lying in a centro-symmetric coordination site [23]. It could also be seen that in DMF solution, the luminescence of europium was quenched which is ascribed to the decomposition of the europium picrate complex in this solvent. In the other three solvents, the europium picrate complex has the similar excitation and emission wavelengths.

In  $\text{CHCl}_3$  solution, the europium picrate complex has the strongest luminescence, followed by acetone and then acetonitrile. This is due to the coordinating effects of the solvents, namely solvate effect [24] where vibrational quenching of the complex excited state may occur through high energy oscillators on the solvent molecule.

The fluorescence quantum yield  $\Phi$  of the europium picrate complex in  $\text{CHCl}_3$  (concentration:  $1.0 \times 10^{-5} \text{ mol L}^{-1}$ ) was found to be  $5.81 \times 10^{-3}$  with quinine sulfate as Ref. [25].

Table 8  
Fluorescence data for the europium picrate complex

Complex	Solvent	$\lambda_{\text{ex}}$ (nm)	$\lambda_{\text{em}}$ (nm)	RFI	assignment
Eu(pic) <sub>3</sub> L	Solid state	451	595	551	$^5\text{D}_0 \rightarrow ^7\text{F}_1$
			614	4233	$^5\text{D}_0 \rightarrow ^7\text{F}_2$
	$\text{CHCl}_3$	463	594	277	$^5\text{D}_0 \rightarrow ^7\text{F}_1$
			615	2260	$^5\text{D}_0 \rightarrow ^7\text{F}_2$
	Acetone	463	594	106	$^5\text{D}_0 \rightarrow ^7\text{F}_1$
			615	453	$^5\text{D}_0 \rightarrow ^7\text{F}_2$
	Acetonitrile	463	594	34	$^5\text{D}_0 \rightarrow ^7\text{F}_1$
			615	92	$^5\text{D}_0 \rightarrow ^7\text{F}_2$
	DMF				

The characteristic luminescence of the terbium picrate complex was not observed, either in solid state or in solutions. The reason is probably that the energy gap between the triplet state levels of the ligand in picrate complex and the lowest resonance level of the europium favor the energy transfer process for europium. In order to acquire the triplet excited state  $T_1$  of the ligand **L** in the picrate complex, the phosphorescence spectrum of the Gd(III) picrate complex was measured at 77 K in a chloroform–methanol–ethanol mixture (v:v:v, 1:5:5). The triplet state energy levels  $T_1$  of the ligand **L** in picrate complex, which was calculated from the shortest wavelength phosphorescence band [26] of the Gd(III) picrate complex, is  $21186\text{ cm}^{-1}$ . This energy level is above the lowest excited resonance level  $^5D_0$  of Eu(III) ( $17300\text{ cm}^{-1}$ ) and  $^5D_4$  ( $20500\text{ cm}^{-1}$ ) of Tb(III). Thus the absorbed energy could be transferred from ligand to the Eu(III) or Tb(III) ions. The triplet state energy level  $T_1$  of this ligand **L** in picrate complex matches better to the lowest resonance level of Eu(III) ( $\Delta\nu = 3886\text{ cm}^{-1}$ ) than Tb(III) ( $\Delta\nu = 686\text{ cm}^{-1}$ ) ion, because such small  $\Delta\nu(T_1 - ^5D_4)$  could result in a back-energy transfer process from the excited resonance level  $^5D_4$  of Tb(III) to the triplet state energy level  $T_1$  of this ligand **L** and quench the luminescence of the Tb(III) picrate complex [27].

In contrast with the strong emission of the europium picrate complex, the europium nitrate complex exhibited weak characteristic emission (the excitation and emission slit widths were 2.5 nm, Fig. 9). The phosphorescence spectrum of the Gd(III) nitrate complex was measured at 77 K in a methanol–ethanol mixture (v:v, 1:1), the triplet state energy levels  $T_1$  of the ligand **L** in the nitrate complex, which was calculated from the shortest wavelength phosphorescence band [26] of the Gd(III) nitrate complex, is  $22075\text{ cm}^{-1}$ . The results indicate that the counter anions of complexes hardly influence the triplet state energy level  $T_1$  of this ligand **L**, but notably affect the fluorescence properties of the europium complexes.

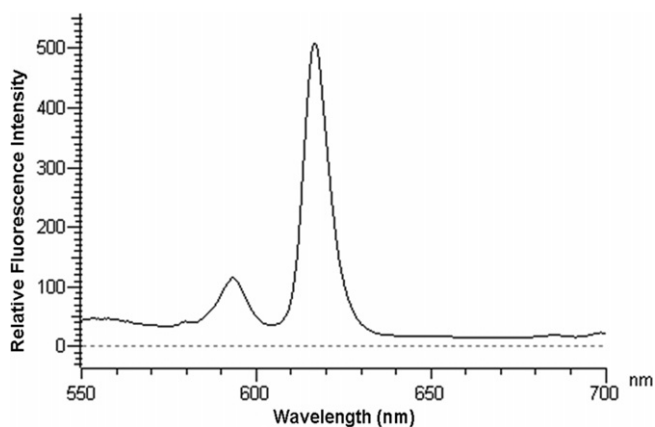


Fig. 9. The emission spectrum of the europium nitrate complex in solid state.

We deduce that this is due to the following three effects. First, the coordinated picrates participate in the energy absorption and transfer process for the Eu(III) ion, make the three-component complex system an optimal state for the luminescence of europium, accordingly enhancing the relative fluorescence intensity of the europium picrate complex. Secondly, the intermolecular  $\pi$ – $\pi$  stacks between picrates favor to the energy transfer for europium. However, the coordinated nitrates do not play these roles like picrates in the europium complex. Thirdly, the non-radiative deactivation of the europium emitting state could quench the luminescence of the Eu(III) nitrate complex [27].

#### 4. Conclusion

In this paper, we reported the preparation, luminescent properties of *N*-phenyl-2-[2'-(phenyl-ethyl-carbamoyl)-methoxy]-biphenyl-2-yloxy)-*N*-ethyl-acetamide (**L**) lanthanide complexes and the supramolecular structures of  $[\text{La}(\text{pic})_3\text{L}]$  and  $2[\text{La}(\text{NO}_3)_3\text{L}(\text{H}_2\text{O})] \cdot \text{H}_2\text{O} \cdot 0.5\text{C}_2\text{H}_5\text{OH}$  which are the assemblies of the complex units via the intermolecular hydrogen bonds and  $\pi$ – $\pi$  stacking interactions. The free ligand is achiral, but it induces axial chirality in the lanthanum nitrate complex, which is directed by the metal ions in the assembly process of the organic ligands with the metal ions. The europium picrate complex exhibited strong characteristic fluorescence whereas the terbium picrate complex showed no luminescence. The lowest triplet state energy level of the ligand in the picrate complex matches better to the resonance level of Eu(III) than Tb(III) ion. The Eu(III) nitrate complex exhibited quite weak characteristic fluorescence. So we can see that the counter anion of complexes is very essential in determining the fluorescent properties of the rare earth complexes. Further studies on the ligand and their complexes are in proceeding.

#### Acknowledgements

We are grateful to the NSFC (Grants 20371022, 20431010 and 20021001), and the Specialized Research Fund for the Doctoral Program of Higher Education (200307300015) for financial support.

#### Appendix A. Supplementary material

CCDC 622187 and 622188 contain the supplementary crystallographic data for lanthanum picrate complex and lanthanum nitrate complex. These data can be obtained free of charge via <http://www.ccdc.cam.ac.uk/conts/retrieving.html>, or from the Cambridge Crystallographic Data Centre, 12 Union Road, Cambridge CB2 1EZ, UK; fax: (+44) 1223-336-033; or e-mail: [deposit@ccdc.cam.ac.uk](mailto:deposit@ccdc.cam.ac.uk). Supplementary data associated with this article can be found, in the online version, at [doi:10.1016/j.poly.2006.12.019](https://doi.org/10.1016/j.poly.2006.12.019).

## References

- [1] S. Faulkner, S.A.P. Pope, *J. Am. Chem. Soc.* 125 (2003) 10526.
- [2] Q. Silvio, M. Giovanni, F. Alessandra, A. Gianluca, B. Francesco, *Inorg. Chem.* 43 (2004) 1294.
- [3] G. Xu, Z.M. Wang, Z. He, Z. Lu, C.S. Liao, C.H. Yan, *Inorg. Chem.* 41 (2002) 6802.
- [4] Q. Li, T. Li, J.G. Wu, *J. Phys. Chem. B* 105 (2001) 12293.
- [5] V. Patroniak, P.N.W. Baxter, J.M. Lehn, Z. Hnatejko, M. Kubicki, *Eur. J. Inorg. Chem.* (2004) 2379.
- [6] B.L. An, M.L. Gong, M.X. Li, J.M. Zhang, *J. Mol. Struct.* 687 (2004) 1.
- [7] Y.-S. Yang, S.-H. Cai, *Hua Xue Shi Ji.* 6 (1984) 133.
- [8] Y.Z. Ding, J.Z. Lu, Y.S. Yang, *Hua Xue Shi Ji.* 8 (1986) 201.
- [9] W. Yang, X.L. Teng, *M. Chem, Talanta* 46 (1998) 527.
- [10] (a) W.S. Liu, X.F. Li, Y.H. Wen, M.Y. Tan, *Dalton Trans.* (2004) 640;  
(b) Y.L. Zhang, W.H. Jiang, W.S. Liu, Y.H. Wen, *Polyhedron* 22 (2003) 1695;  
(c) Y.L. Zhang, W.S. Liu, W. Dou, W.W. Qin, *Spectrochim. Acta, Part A* 60 (2004) 1707.
- [11] Y.C. Tian, Y.Q. Liang, J.Z. Ni, *Chem. J. Chin. Univ.* 9 (1988) 113.
- [12] L.-Y. Fan, W.-S. Liu, X.-M. Gan, N. Tang, M.-Y. Tan, W.-H. Jiang, K.-B. Yu, *Polyhedron* 19 (2000) 779.
- [13] W.J. Gear, *Coord. Chem. Rev.* 7 (1971) 81.
- [14] C. Janiak, *Dalton Trans.* (2000) 3885.
- [15] B. Wu, D. Yuan, F. Jiang, R. Wang, L. Han, Y. Zhou, M. Hong, *Eur. J. Inorg. Chem.* (2004) 2695.
- [16] G.R. Desiraju, *Chem. Commun.* 24 (2005) 2995.
- [17] S.X. Liu, W.S. Liu, M.Y. Tan, K.B. Yu, *J. Coord. Chem.* 10 (1996) 391.
- [18] W. Carnall, S. Siegel, J. Ferrano, B. Tani, E. Gebert, *Inorg. Chem.* 12 (1973) 560.
- [19] K. Nakamoto, *Infrared and Raman Spectra of Inorganic and Coordination Compounds*, third ed., John Wiley, New York, 1978, p. 227.
- [20] X. Mao, L.F. Shen, J.Z. Ni, *Bopuxuezazhi* 1 (1985) 201.
- [21] (a) C.K. Jorgensen, *Prog. Inorg. Chem.* 4 (1962) 73;  
(b) S.P. Sinha, *Spectrochim. Acta* 22 (1966) 57;  
(c) D.E. Henrie, G.R. Choppin, *J. Chem. Phys.* 49 (1968) 477.
- [22] A.K. Solanki, A.M. Bhandaka, *J. Inorg. Nucl. Chem.* 41 (1979) 1311.
- [23] M. Albin, R.R. Wright Jr., W.D. Horrocks, *Inorg. Chem.* 24 (1985) 2491.
- [24] H.Q. Liu, T.C. Cheung, C.M. Che, *Chem. Commun.* (1996) 1039.
- [25] (a) C.A. Parker, W.T. Rees, *Analyst* 85 (1960) 587;  
(b) W. Yang, Z.L. Mo, X.L. Teng, M. Chen, J.Z. Gao, L. Yuan, J.W. Kang, Q.Y. Ou, *Analyst* 123 (1998) 1745.
- [26] W. Dawson, J. Kropp, M. Windsor, *J. Chem. Phys.* 45 (1966) 2410.
- [27] F. Gutierrez, C. Tedeschi, L. Maron, J.-P. Daudey, R. Poteau, J. Azema, P. Tisn'es, C. Picard, *J. Chem. Soc., Dalton Trans.* (2004) 1334.